Settlement Prediction due to Diaphragm Walls Installation at Heliopolis Metro Station in Cairo, Egypt

Hussein M. Mostafa[*1], Hatem M. El-ssayed[2] and Safiya M. Hassan[3]

1. *Soil Mechanics Lecturer at Civil Engineering Dept., Faculty of Engineering, Helwan University, Cairo, Egypt, email: hussain_moustafa@m-eng.helwan.edu.eg.*
2. *Project Manager at IESCO Geo-engineering and Mining Consulting, Cairo, Egypt.*
3. *Assistance Professor at Department of Mineral Resources, Faculty of Earth Science, Beni-Suef University, Beni Suef, Egypt..*

Abstract. This paper presents a case history in Heliopolis, Egypt which is an underground metro station serving a high densely populated area in northeastern Cairo. This station was planned to maintain and attract density population (job-housing) in the nearby areas. The tunnel excavation and the constructed station resulted in a lateral soil displacement component and a reverse pressure affecting the side supporting system along the station sections. This displacement depends on many factors such as soil profile, subsoil properties, depth of excavation inside the diaphragm walls (D-walls), type and stiffness of supporting system, time period of construction, surrounding structures, and surcharge loads. The present paper is comparing the observed horizontal displacement data (more than 2 years monitoring) with the corresponding estimated values of the soil model for detecting the deviation in predicted settlements in the long run and for the evaluation of any hazardous damages on buildings near excavations. It is concluded that the horizontal displacement behind the wall is about 0.06% of the excavation depth and the surface settlement is about 6 – 24% of the horizontal displacement behind the wall if all construction stages are included. Also, the surface settlement is about 0.004 – 0.014% of the excavation depth of the underground station.

Keywords: Deep Excavation, Vertical Displacement, Horizontal Displacement, Settlement, and Heliopolis.

1. Introduction

The reduction of overground spaces in big cities leads to a complicated traffic system and a complex mobility transportation flow. To overcome the traffic problem and to increase the usable underground spaces in Cairo city, engineers have involved in the underground constructions. This reduced the load over ground and optimized the expensive cost in the urban cities. Cairo is considered one of the largest and most crowded cities not only in Egypt but also in the world. Cairo Metro Line 3 (CML3) is extended from Imbaba to Cairo Airport; Phase-4A of the CML3 extends from Heliopolis Station to the Exit Shaft with a total length of about 5.1 km. Fig. 1 shows the general layout of Heliopolis Station (our case study).

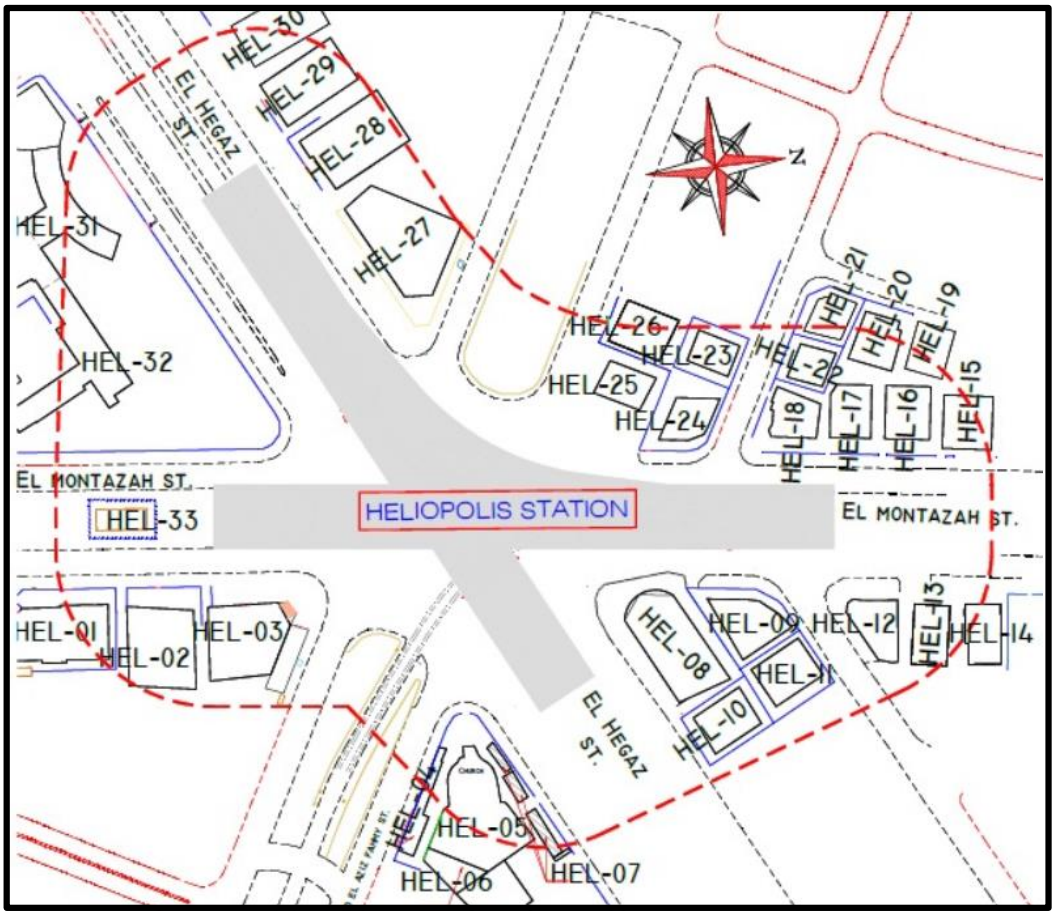

Fig. 1 The general layout of Heliopolis Station, after (EFJV, 2015).

In the tunneling process generally, engineers do their best to control the ground surface settlements resulted from the excavation. The main goal usually in this case is restricted to avoiding the excavation collapse (Suwansawat et al 2006; and Zahid et al 2021). The determination of the maxim ground surface settlement is helping in the estimation of the required input factors non-linearly in multitarget observations. However, the stability results are depending on the reliability of the soil mechanical simulation model.

In urban areas, deep excavations are frequently located very near to existing buildings. They often cause unexpected movements which could cause harmful damage to the adjacent properties. The movements of the installed retaining walls and their surrounding grounds have been studied by too many researchers (e.g., Peck 1969; Hsieh et al 2003; Khoiri and Ou 2013; and Koh and Chua 2013). Researchers mainly constructed their models depending on the finite element method in calculating the subsurface ground variations due to excavation.

Field measurements give approval that ground movement resulting from diaphragm wall installation could be a significant component of the total soil displacement (Tedd et al 1984; and Siavash et al 2016). A new method was combined

with a 3-D nonlinear analysis and a constitutive model determining bulk and shear modulus variations, depending on the stress loading numerical scale (Comodromos, et al 2013). It has been observed that the most significant effect in front of a given panel happened at the beginning of the installation process. The lateral movements faced any other subsequent panels is limited.

Hsiung and Dao (2015) stated that a better prediction of the ground surface settlements can be obtained as an advanced constitutive model of soil that takes into account small strain characteristics of soil is adopted in the numerical analysis. For obtaining better results, the establishment of a constitutive model of soil enables engineers in prediction of the ground surface settlements by taking into account the small strain characteristics of soil numerically. However, the input parameters of such preliminary models of soil have to be derived from complicated testing.

The authors in the current study tested the applicability of their predicted model for estimating the ground movements and comparing it with the resulted observed data. As a result of the unexpected observed (measured) deflection values in the diaphragm walls, they recommend a detailed characterization of the soils for detecting the subsoil structures. This will define completely failure zones of soils and will resist any future damage in the Heliopolis Station which in turn reduces hazardous effects.

2. Deep excavation case history

2.1. Project Description.

The project comprises the following components as per EFJV company (2015):

a) Underground stations: They extend from Haroun El Rashid Station (KP 10.592111) to TBM Exit Shaft (KP 5.487), passing through Heliopolis Square Station (KP 9.771784), Alf Maskan Station (KP 8.637830), Al Shams Club Station (KP 7.430608), and El Nozha-1 Station (KP 6.244138). The length of each station ranges from 151 m to 223 m.
b) Underground tunnel: This tunnel is executed by Tunnel Boring Machine (TBM). The tunnel is circular in shape with an internal diameter of 8.35 m.
c) Four annex structures: These structures are performed to work as ventilation rooms for the bored tunnel.
d) Inclinometer devices: These inclinometers were fixed in specific locations along the diaphragm wall itself and beneath the adjacent structures in the soil piles behind the wall. This enabled us to measure the total horizontal displacement of the wall-soil system. Intensive work was done for measuring the settlement of soil and properties along the specified points.
e) Elevation Reference Points (ERPs): For measuring the vertical displacement of soil occurred due to the excavation and happened beneath the nearby properties in the zone of influence. The zone of influence was taken as twice

the excavation depth, with a minimum of 57 meters all around the D-wall perimeter.

Heliopolis Station is located along El Montazah Street in Cairo. The station consists of two intersecting rectangular each has dimensions of about 225 m x 23 m. The depth of the excavation is about 28.5 m below street level.

2.2. Site and Subsurface Conditions.

Based on the site investigation, the soil stratigraphy was explored; the excavation was in the eastern part of the Greater Cairo City at Heliopolis square region. The depth of the excavation for Heliopolis subway station was about 29m and it was reported as a sand deep excavation case. The site investigation also detected that the groundwater level was ranging between 27.9m and 28.3m deep below the ground surface. The geology of Cairo is characterized by tertiary sedimentary soils and quaternary soils, both are setting at the top of older basement rocks.

The studied structures are Hel-02, Hel-8, Hel-09, Hel-18, Hel-23, and Hel-25. The age of these structures is ranging from 2 years to 50 years at the date of inspection (January 2016). The number of stories of these structures is ranging between 2 floors to 12 floors. The related design sections of Heliopolis station are including only the buildings which are related to design sections: A, A/, B, B/, C, D, D/, E, E/, F, G, H, and I as shown in Fig. 2. Two boreholes (BH104D and BH103D) were drilled for detecting the soil profile in the excavation area. Fig. 3 is displaying the location of both wells. They represent well-defined and very similar sequences of sedimentary facies as indicated by Fig. 4. Five major sedimentary units are defined in our sections based on lithostratigraphy. Each sedimentary unit is characterized by its own lithology and lithological succession; the litho-types defined sedimentary units as follows:

i) Unit I: (Fill layer)

This unit is a fill layer which appears at the ground surface and extends to a depth of 2.0m in borehole BH-104D. It is composed of asphalt pavement, limestone pieces and followed by a mixture of gravel and sand. The thickness of this unit is decreased in the borehole BH-103D to become 1.15m and it is characterized by the same composition but gravel is presented as limestone pieces.

ii) Unit II: (Sand and Gravel layer)

This unit is consisting of 1.25m (from 2.0m to 3.25m) in borehole BH-104D forming a mixture of sand and gravel with traces of silt. However, this unit increased in thickness in borehole BH-103D from 1.15m to 10.5m and it varies in composition where its mixture is dominated by gravel more than sand.

iii) Unit III: (Sand Layer)

This unit is composed of 7.7m (from 3.25m to 10.95m) in borehole BH 104D of

very dense fine to medium sand with some gravel and silt. The silt layer starts from 9.0m to 9.15m. However, this unit decreased in thickness laterally in borehole BH-103D to become 3.7m (from 10.5m to 14.0m). This unit is identical in composition to borehole BH-103D.

iv) Unit IV: (Clay layer)

This unit is measured 5.85m (from 10.95m to 16.8m) in borehole BH-104D and it is composed of very stiff to hard silty clay with fragments of limestone and gravel. This unit is increasing laterally in borehole BH-103D to become 7.6m (from 14.0m to 21.6m) with the same composition.

v) Unit V: (Sand layer)

This unit has a thickness of 25.2m (from 16.8m to 42m) in borehole BH-104D from very dense fine to medium sand including various percentages of silt. The sand contains various percentages of gravel at depths ranging from 28.0m to 42.0m. Moreover, this unit is increasing laterally in BH-103D to become 49.0m in thickness from 21.6m to 70.6m displaying the same composition.

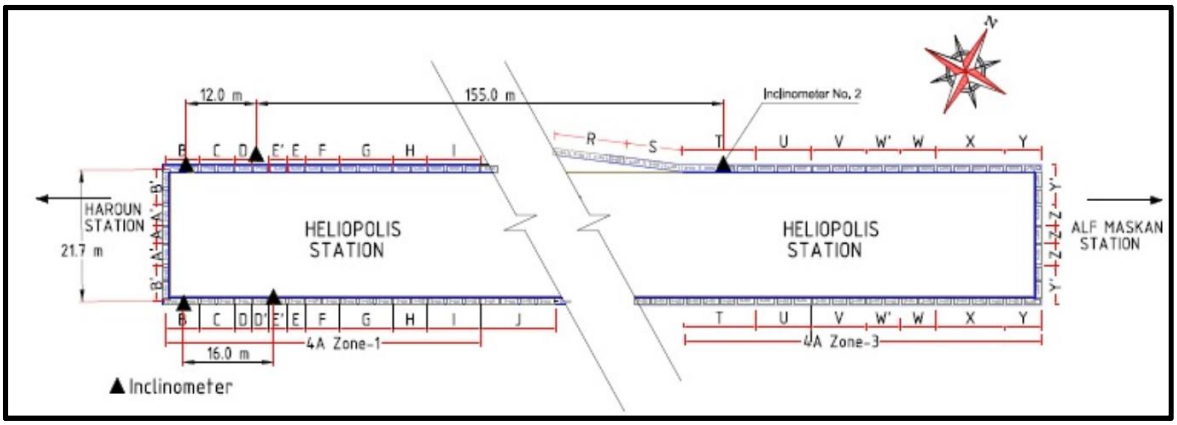

Fig. 2 The design sections and inclinometers' locations along the investigated site. (after EFJV 2015)

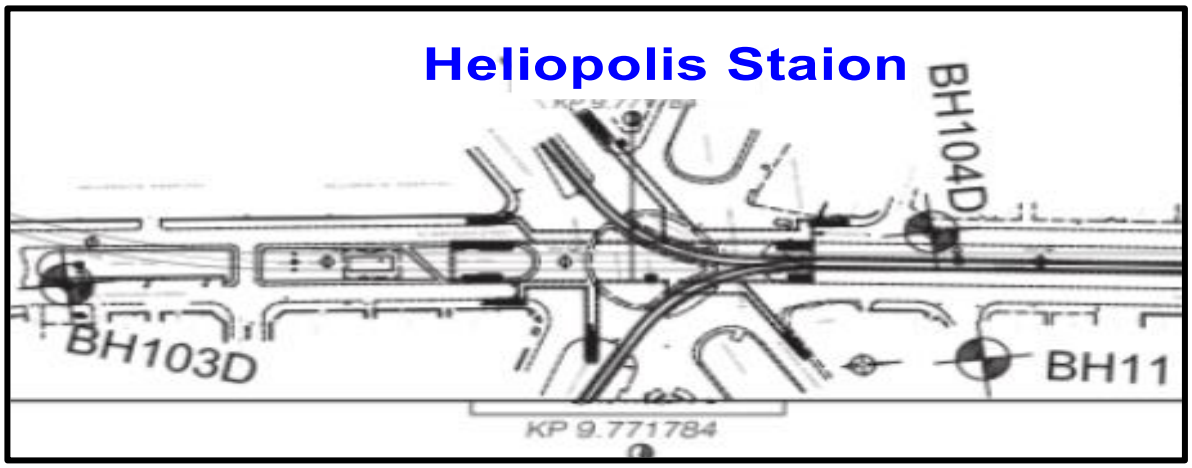

Fig. 3 The locations of the two boreholes BH-103D and BH-104D. (after EFJV 2015)

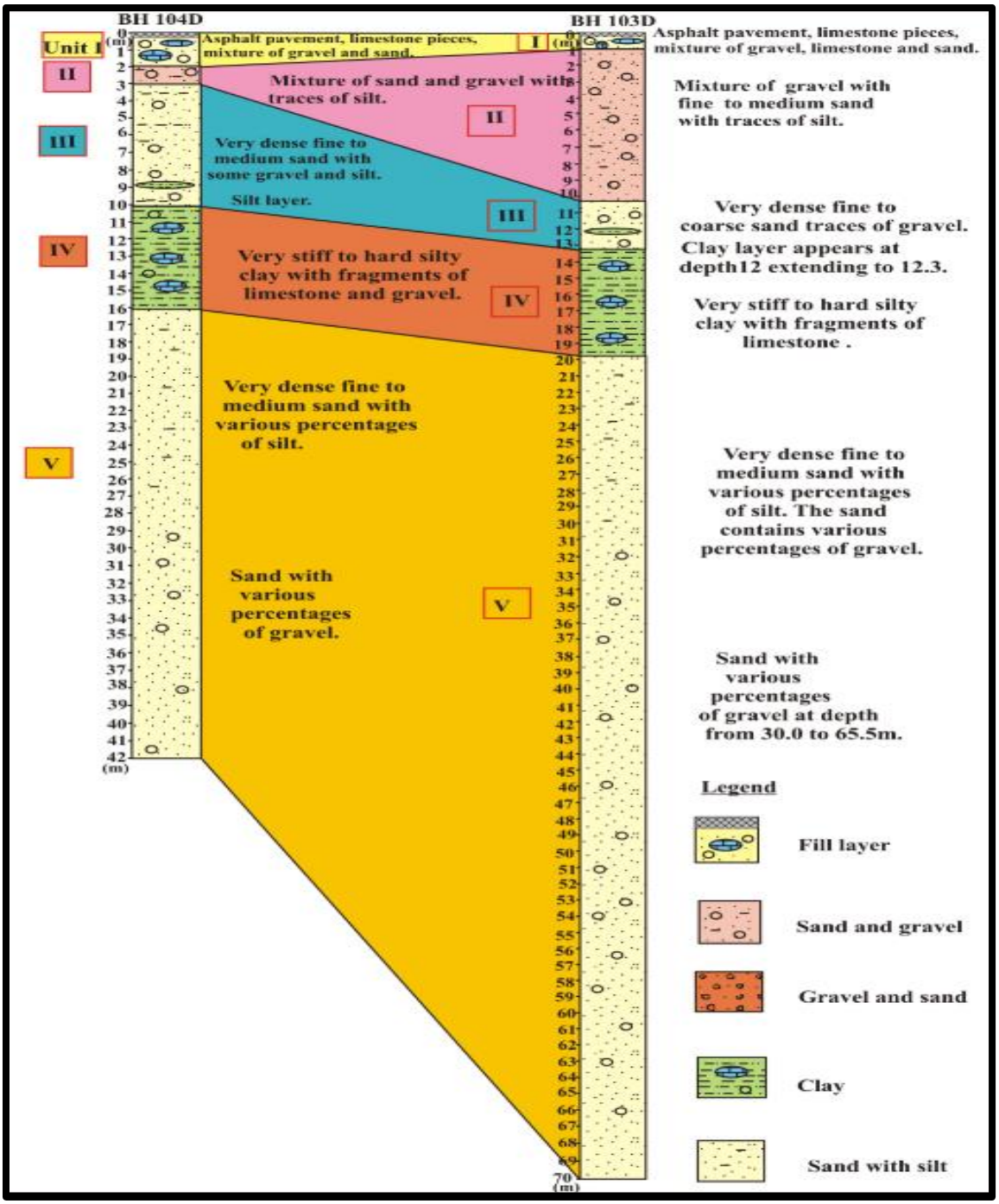

Fig. 4 Lithostratigraphy of Heliopolis Square to Alf Maskan Station.

2.3. Design Soil Parameters.

Based on the site investigation program, the design shear and stiffness parameters for the soil strata encountered in the boreholes are presented in Table 1.

Table 1 Recommended Design Soil Parameters – Heliopolis Station. (after EFJV 2015)

Layer	Bulk density (kN/m^3)	Layer top (m)	Layer bottom (m)	Ko	Undrained Parameters			Drained Parameters			
					Cu (kPa)	Eu (MPa)	ν_u	C' (kPa)	ϕ' (^{o})	E' (MPa)	ν'
Fill	18	0.0	-2.0	0.55	-	-	-	0	27	10	0.3
Upper Sand	19	-2.0	-14.0	0.40	-	-	-	0	37	50	0.3
Clay	19	-14.0	-34.0	0.80	200	30	0.45	15	29	27	0.35
Lower Sand	21	-34.0	-50.0	0.36	-	-	-	0	>40	120	0.3

3. Measured and predicted data

3.1. Measured Data at the Construction Site.

It worth to mention that the measured data is obtained from EFJV company. However, the predicted (theoretical) results of settlements were mainly determined based on the calculated horizontal displacement values of the D-wall which were made by EFJV Design Office. The Plaxis software was used for modeling the soil-structure interaction (Plaxis, 2016).

The studied structures included in the current study which are located within the station influence zone were six (6) buildings. The Elevation Reference Point (ERP's) method was applied to six buildings in the influence zone which are Hel-02, Hel-08, Hel-09, Hel-18, Hel-23, and Hel-25. Several inclinometers were fixed at the soil and along the diaphragm wall for calculating the horizontal displacements which generated in soil and at the retaining wall, Fig. 2. The collected data were evaluated to determine the buildings settlements that are related to the diaphragm wall installation and the excavation process. The measured movements were plotted versus time for observing the soil behavior with time. The time-displacements plots of different elevation reference points for the above-mentioned properties are displayed by Figs. 5 and 6.

In the pre-drilling stage, raising the ground level close to the edge of the excavation will produce the largest impact on the top layers, thus resulting in losing capturing parts of the ground surface displacements due to the construction process. The vertical displacement at larger depths is very important, particularly for buildings with deep foundations. This may be due to the decrease of the influence zone two times smaller than the excavation depth approximately (Aye et al. 2006).

The monitored displacements in the current study were started in August, 2016 and ended in May, 2019 (more than 2 years). The recorded data were varied from building to building and also from point to point for the same building. For example, the settlements at point "B" for Hel-02 are reflecting a little increase of subsidence with time, Fig. 5a, while there is an obvious increase in displacement at corner "A" of Hel-2 building. Corner point "C" in Hel-23 displayed a variation of displacement which

started in May 2017 and continuously grown with time, Fig. 6b. In case of building Hel-09, there is stability in the settlement after Nov., 2018 at the points “A, B and C”, Fig. 5c.

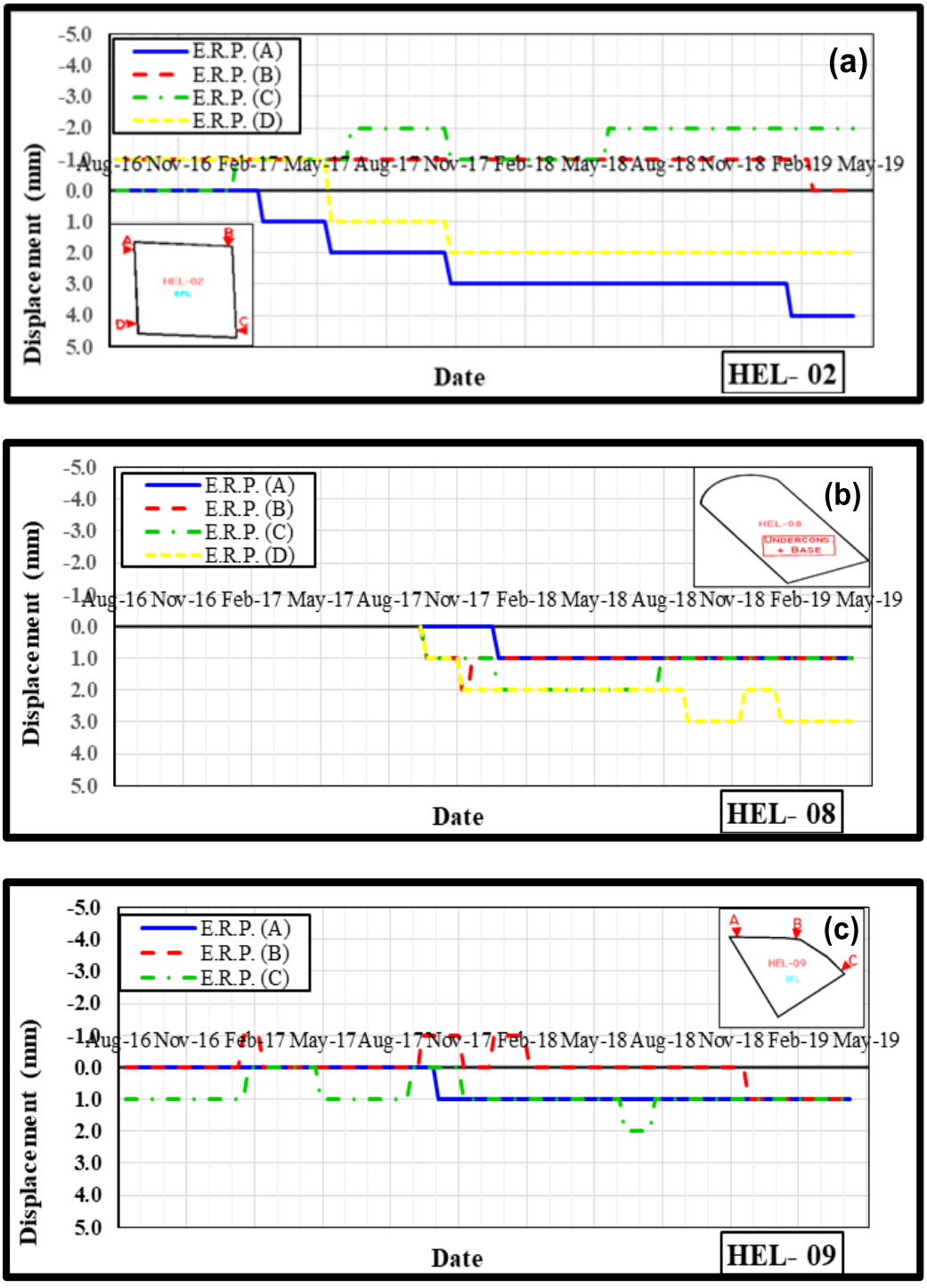

Fig. 5 Time-displacement relations for the monitored elevation reference points for: a) Hel-02, b) Hel-08, and c) Hel-09 buildings.

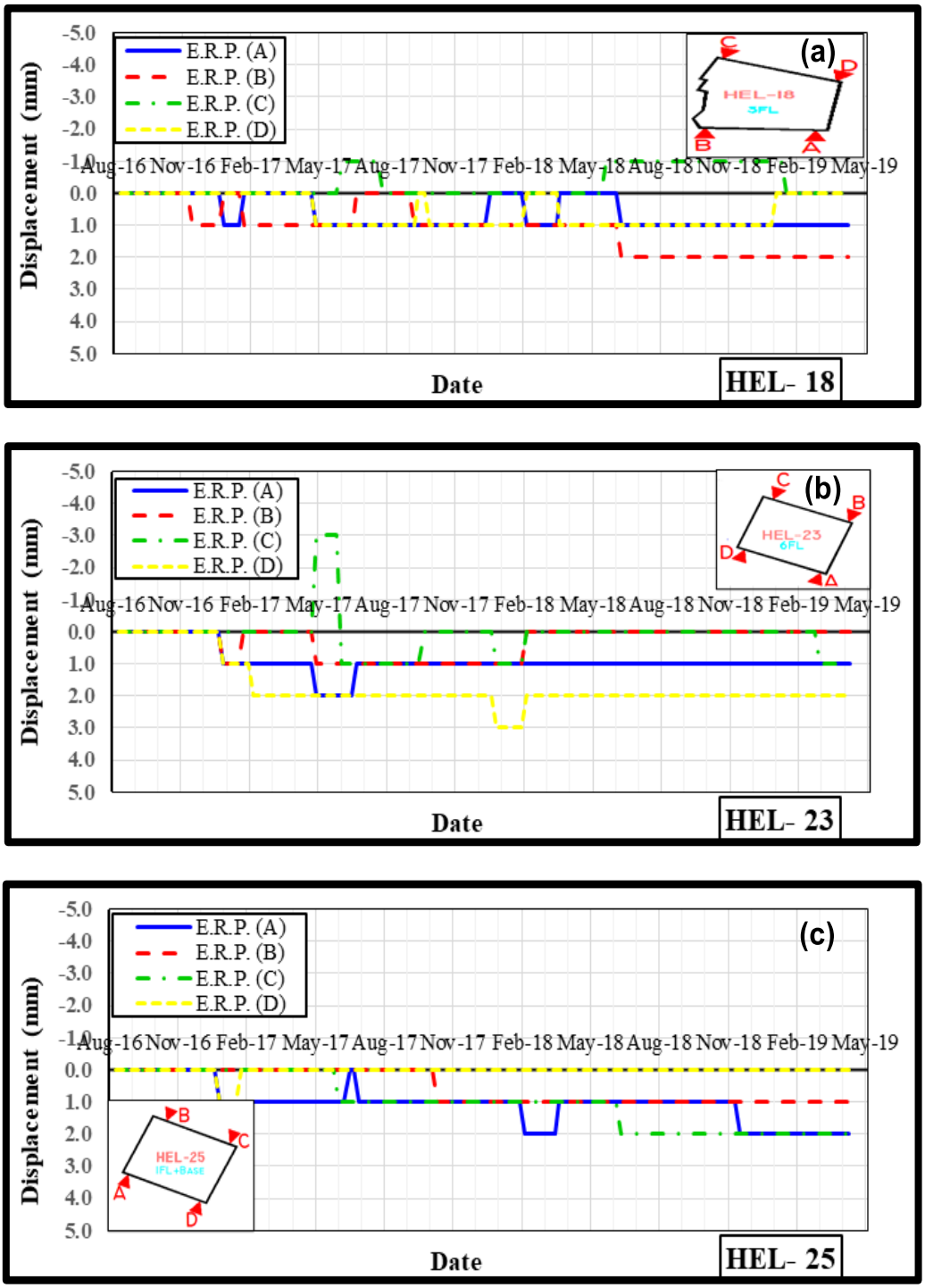

Fig. 6 Time-displacement relations for the monitored elevation reference points for: a) Hel-18, b) Hel-23, and c) Hel-25 buildings.

This gives us an indication that properties such that Hel-2, Hel-8 and Hel-23 have to be tracked in the long run for the existence of cracking. On the contrary, Hel-09 has no problem and has not affected by the excavation process. The fluctuations of the settlement values at “A, B and D” corners of Hel-18 need to be investigated for

detailed soil characterization, Fig. 6a. It shows variable amplitudes of displacement which may affect the stability of the property with time. C and D corners of Hel-23 reflect another sinusoidal settlement curve, Fig. 6b. Unlike Hel-18 and Hel-23 as shown in Fig. 6c, the building Hel-25 has a stability of settlement after Nov. 2018.

3.2. Conceptual Basis for the Predicted Data.

The assessment of ground settlements associated with the installation of the diaphragm walls in braced deep excavations became an important step in recent projects. The determination of the major factors affecting the development process contemplates reliable prediction models for settlements. Analyzing data with the aid of mathematical representation facilitates understanding its statistical behavior and enables the prediction of unknown values. The subsurface soil properties, the foundation type, the depth of the adjacent buildings, excavation steps, and the stiffness of the retaining walls are belonging to the above-mentioned factors (Abdel-Rahman and El-Sayed, 2009).

The total settlement can be expressed as the sum of the calculated settlement due to trenching (diaphragm wall) installation ($S^{trenching}$) and the estimated settlement due to excavation procedures ($S^{pitexcavation}$) as follows (Peck, 1969):

$$\mathbf{S^{total} = (S^{trenching}) + (S^{\ pit\ excavation})} \quad (1)$$

Where,

$S^{trenching}$ is the settlement at a distance "x" from the diaphragm wall

$S^{\ pit\ excavation}$ is the maximum settlement at the trench location

We can obtain $S^{trenching}$ from the following equation:

$$\boldsymbol{S^{trenching} = S_{max}^{trenching}\left(1 - \frac{x}{2d}\right)^{m}} \quad (2)$$

Where,

$\boldsymbol{S_{max}^{trenching}}$ is the maximum settlement at the trench location,

x is the distance from the trench,

d is the excavation depth, **m** is 5.

The settlement resulting from pit excavation **($S^{pit\ excavation}$)** is determined as:

$$\boldsymbol{S^{pit\ excavation} = S_{max}^{pit\ excavation} e^{\left(\frac{-x^2}{2(K.H)^2}\right)}} \quad (3)$$

Where,

$\boldsymbol{S_{max}^{pit\ excavation}}$ is the maximum settlement at the wall place,

K is a dimensionless factor; **H** is the final excavation depth.

The settlement envelop can be determined by adding both the trench settlement ($\boldsymbol{S^{trenching}}$) to the pit excavation settlement ($\boldsymbol{S^{pit\ excavation}}$) as expressed in equation (1).

3.3. Parameters for the Estimation of Settlements due to the D-walls.

The application of field procedure skills enables the designer for the estimation of the predicted values of the parameters related to the ground settlements due to excavation inside D-walls. The maximum and minimum numbers for every structure were determined. The following can be postulated:

a. The settlement ratio ***Rs*** (= max. settlement / max. deflection) can be taken as **1.7**.
b. The volume ratio $\boldsymbol{R_v}$ (= volume of the settlement trough / volume of lateral deformed shape for D-wall) can be taken as **0.6**.
c. The ratio between the predicted and measured settlement ($\boldsymbol{S_{act}}$ **/** $\boldsymbol{S_{pre}}$**)** can be assigned the number **0.3**.

3.4. Finite Elements Analysis.

The analyses mainly were based on the linear Mohr-Coulomb soil parameters as the Mohr–Coulomb model and the Drucker–Prager model are the most widely used models (Naseri et al 2021; Liu, et al 2021; and Kechidi et al 2021).

The parameters were determined from the soil investigation program of the station.

A numerical analysis, in the current study, was carried out using the two-dimensional finite element program Plaxis 2D. The different soil layers were modeled using fifteen-node triangular elements. The adopted finite element mesh consisted of 29061 nodes and 3514 finite elements. The boundary conditions were adopted as follows: vertical boundaries have zero lateral movements, i.e. roller support, and were considered to be impermeable. The bottom horizontal boundary was restrained vertically and horizontally and was considered to be permeable, modeling a sand formation. A fine mesh option was considered for the entire mesh. Moreover, the zone around diaphragm walls was locally refined. The elasto-plastic Mohr-Coulomb model was used to simulate the behavior of the soil layers using the parameters listed in item 2.3.

Plate elements had been selected to simulate the diaphragm walls, roof and raft. Plate element is a thin structural element defined by means of stiffness. Table 2 summarize input parameters for Dwalls as follows:

Table 2 Plate elements parameters.

Element	Thickness, d (m)	EI ($kN.m^2/m$)	EA (kN/m)
Diaphragm Wall	1.2	3.02E6	25.20E6
Raft / Roof	1.5	5.91E6	31.50E6

The geometry configuration of the studied model is shown in Fig. 7 as follows:

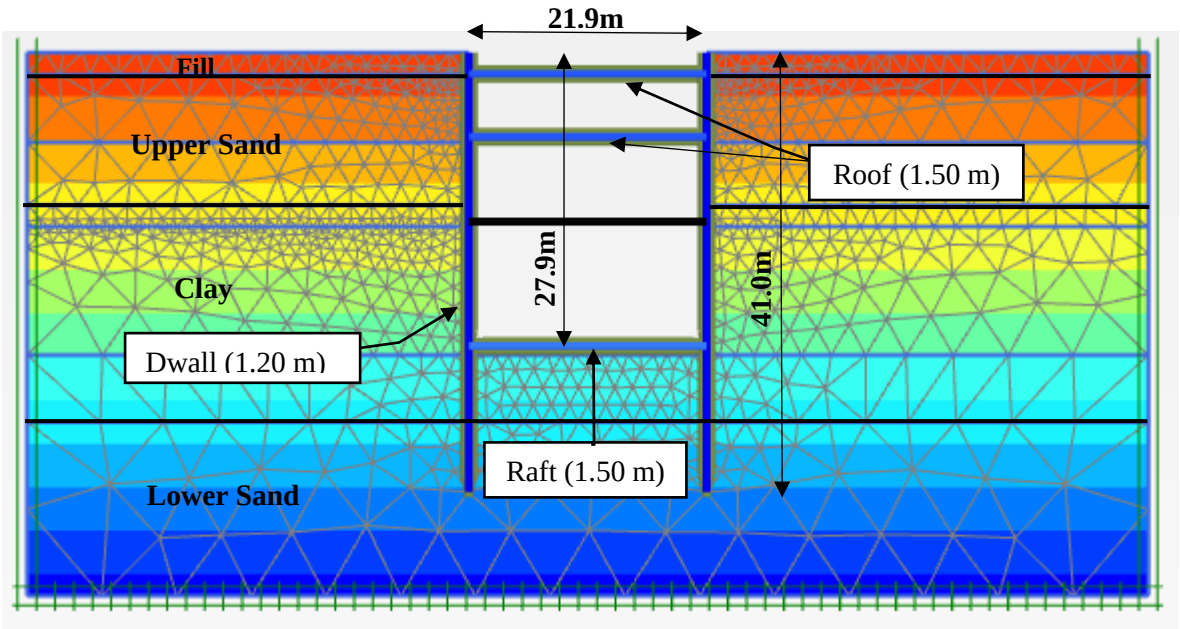

Fig. 7 Model configuration and mesh

3.5. Predicted Settlement and Rotation.

The studied structures included in the current study which are located within the station influence zone were six (6) buildings and their rotations and the predicted maximum settlements are shown in Table 3. Some of these structures have no problem and had not affected by the excavation and the diaphragm process. The selection of the studied structures was based on the location of the D-wall inclinometers for the best correlation between the predicted and the measured data for the studied area.

Table 3 List of buildings which are included in the current study.

Buildings	Max. Predicted Settlement (mm)
HEL-02	21.9
HEL-08	19.8
HEL-09	23.3
HEL-18	23.4
HEL-23	0.4
HEL-25	6.6

4. Results and discussions

The diaphragm wall is considered one of the most important parts of the pit closure system because it is responsible for the resistance of the earth pressures caused by soil removal. The precise design of the embedded wall in turn is necessary for

avoiding pit instability and for the reduction of the construction cost. The numerical simulation can add in changing and adjusting the insertion ratio of the wall which refers to the height of the wall below the pit to the excavation depth (Feng et al. 2022).

Based on Mindlin Solution, the study of the vertical displacement near the wall trench area reveals that the vertical displacement displays a shape funnel-like shape and it has a maximum value located at the center of the excavation. In comparison, the settlement curve itself represents a spoon like-shape and the maximum value is located at a certain distance from the trench (Zhu 2021).

In reality, a structure will undergo both lateral deformations and angular distortion during the excavation process. Hence, we can estimate the influence of the excavation on the adjacent environment as well as the nearby structures surrounding the area. For the Heliopolis station, a 1.2 m thick reinforced concrete diaphragm wall was designed as an earth retaining structure. Figs 8 and 9 show the comparisons of the wall deflections obtained from the field measurements, at the soil and Dwall inclinometers No. (2) in different times with the predicted ones.

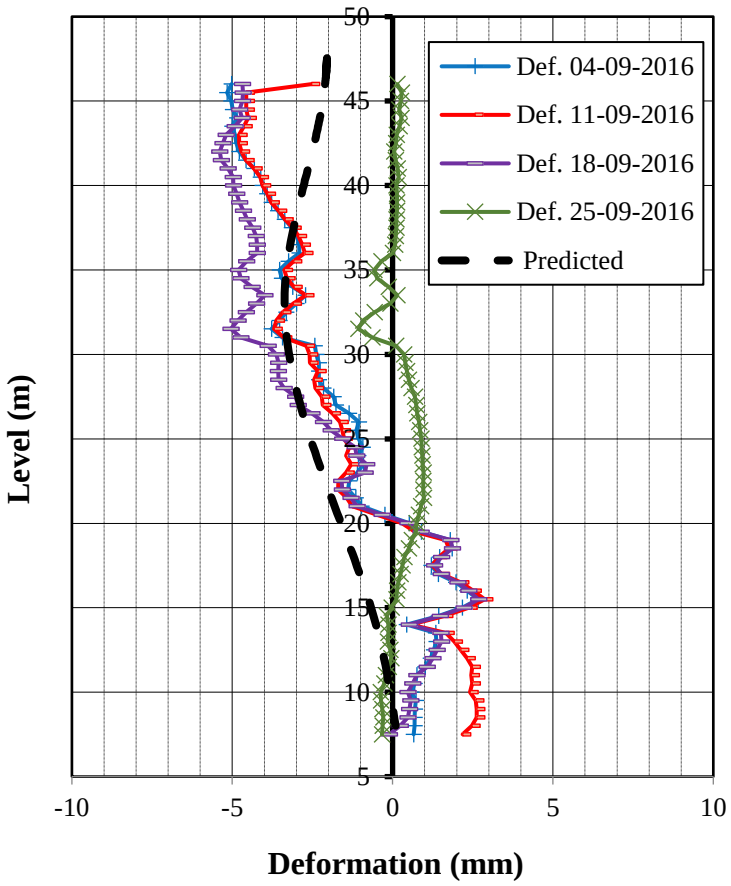

Fig. 8 Wall deflections along the long side of excavation at inclinometer (2) for the year 2016.

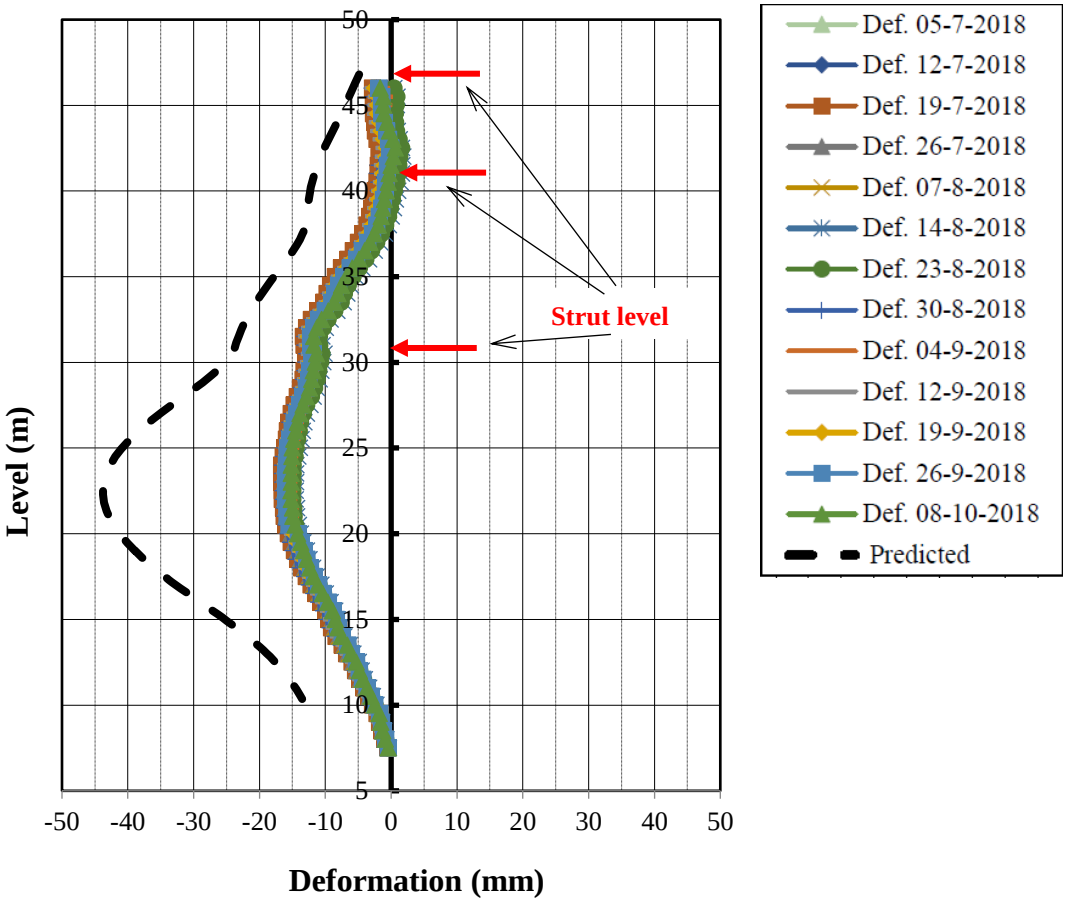

Fig. 9 Wall deflections along the long side of excavation at inclinometer (2) for the year 2018.

As it can be noticed from Figures (8 and 9), the wall behaves as a cantilever at the first stage of excavation because the struts were not introduced yet. The wall is displaying inward movements with depth at subsequent stages of excavation. Time varies from the year 2016 and the year 2018 of excavation. It is clearly seen in Fig. 9 that, the wall deflections obtained in a time close to the end of excavation look like the predicted data. At the initial stages during the year 2016 the deflection values were small (less than 5mm). As we move to the year 2018, the maximum measured deflection appeared clearly at the depth 24.0m in the dense sand layer reaching 17mm, Fig. 9.

For the final stage of excavation at year 2018, the predicted data are conformable with the measured ones in the upper and lower parts of the D-wall and it varies in the central part. The main reason could be related to the fact that the model adopted in current study use only a single Young's modulus, which does not differentiate between loading and unloading.

In addition, the soil properties depend on additional factors such as the subsurface soil structures which could increase or decrease the values of the lateral earth pressure and consequently the resulted lateral displacements of the wall. The slight increasing

amount of deflections reflects a differential change in soil properties at that level and drive the attention to a change in the lateral earth pressure related to that depth.

It worth to mention that due to the relative significant difference between the measured and modeled Dwall deflections, the authors are highly recommending to use the hardening soil model as a good representative model to consider the loading and unloading behaviors instead of Mohr–Coulomb model.

From Fig. 9, it can be concluded that the ratio between the max. horizontal displacement of Dwall (17mm) to the max. excavation depth (27.9m) is about 0.06%. Also, a comparison between the maximum measured settlements and the predicted ones is shown in Table 4.

Table 4 Comparison between measured and predicted settlement.

Buildings	Max. Actual Settlement (mm)	Max. Predicted Settlement (mm)	Actual / Predicted Settlement	% Max. settlement / horizontal displacement	% Max. settlement / depth of excavation
HEL-02	4	21.9	0.18	24	0.014
HEL-08	3	19.8	0.15	18	0.011
HEL-09	1	23.3	0.04	6	0.004
HEL-18	2	23.4	0.09	12	0.007
HEL-23	2	0.4	5.0	12	0.007
HEL-25	2	6.6	0.3	12	0.007

From the previous table, it is obvious that the surface settlement is about 6 – 24% of the horizontal displacement behind the wall if all construction stages are included. Also, the surface settlement is 0.004 – 0.014% of the excavation depth of the pit.

5. Conclusions

A successful installation of retaining walls essentially requires an accurate prediction of the upcoming deformations of the vicinity buildings and the adjacent buried utilities. The degree by which we can trust the predicted settlement is depending on the type of data that combined to form its model no matter if it was a set of equations or numerical models. The analyses mainly were based on the linear Mohr-Coulomb soil model using Plaxis software.

The collected data were evaluated for determining the buildings settlements which are related to the diaphragm wall installation and the excavation process. The measured settlements were piloted versus time for observing the soil behavior with time. The Elevation Reference Point (ERP's) method was applied to six buildings in the influence zone which are Hel-02, Hel-08, Hel-09, Hel-18, Hel-23, and Hel-25 to monitor the movements of buildings. The time-displacements plots of different elevation reference points for the above-mentioned properties were displayed. The maximum deflection appeared clearly at the depth 24m in the dense sand layer

reaching 17mm. This could reflect a significant increase in the wall deflection causing a substantial damage on it.

In case of Heliopolis project, there is a major variation in the deflection curve of the diaphragm wall at the inclinometer (2) between the year 2016 and the year 2018 marking a change in the lateral pressure around the mid-section of the wall.

It is concluded that the horizontal displacement behind the wall is about 0.06% of the excavation depth and the surface settlement is about 6 – 24% of the horizontal displacement behind the wall if all construction stages are included.

The measured settlements are not contributing a real problem right now on Heliopolis Station but it may be appeared to be harmful in the long run. The current study is worthy challenge when it comes to other stations which already display a tremendous increase in the value of the surface loading as a result of the new constructed engineering projects.

Acknowledgements

The authors are indebted to the staff of the Egyptian French Joint Venture Company (EFJV) and the National Authority of Tunnels (NAT) for their continuous help and for the data supply.

References

Suwansawat, S. and Einstein, H.H. (2006), "Artificial neural networks for predicting the maximum surface settlement caused by EPB shield tunneling", *Tunneling and Underground Space Technology*, **21**(2), 133–150. https://doi.org/10.1016/j.tust.2005.06.007.

Zahid U.R., Sajjad H., Muhammad T., Noor M., Saira S., Nasrullah D. (2021), "Prevention and Mitigation Management of Tunnel Collapse and Failure during Construction-A Review", *Int. J. Econ. Environ. Geol.*, **12**(2), 72-79. https://doi.org/10.46660/ijeeg.Vol12.Iss2.2021.590.

Peck, R.B. (1969), "Deep excavation and tunneling in soft ground", *Proceedings of the Seventh International Conference on Soil Mechanics and Foundation Engineering*, Mexico Instituto of Engineering, Mexico City, Mexico, August, 225–290.

Hsieh, P.G., Kung, T.C., Ou, C.Y. and Tang, Y.G. (2003), "Deep excavation analysis with consideration of small strain modulus and its degradation behavior of clay.", *Proceedings of the 12th Asian Regional Conference on Soil Mechanics and Geotechnical Engineering*, Singapore, August.

Khoiri, M. and Ou, C.Y. (2013), "Evaluation of deformation parameter for deep excavation in sand through case studies", *Computers and Geotechnics*, **47**(1), 57-67, https://doi.org/10.1016/j.compgeo.2012.06.009.

Koh, E. and Chua, T.S. (2013), "Multi earth retaining systems for an excavation project in Old Alluvium, Singapore.", *International Symposium on Advances in Foundation Engineering*, Singapore, January.

Tedd, P., Chard, B.M., Charles, J.A. and Symons, I.F. (1984), "Behaviour of a propped embedded retaining wall in stiff clay at Bell Common Tunnel", *Geotechnique*, **34**(4), 513-32, https://doi.org/10.1680/geot.1984.34.4.513.

Siavash K.B., Ashkan G.N., Alborz H., (2016) "Study on horizontal displacement of restrained excavation walls by cantilever retaining wall", *IJESRT*, **5**(6), 847-852, https://doi.org/10.5281/zenodo.56029.

Comodromos, E.M., Papadopoulou, M.C. and Konstantinidis, G.K. (2013), "Effects on adjacent buildings from diaphragm wall installation.", *Proceedings of the 18th International Conference on Soil Mechanics and Geotechnical Engineering*, Paris, France, September.

Hsiung, B.C.B. and Dao, S.D. (2015), "Prediction of ground surface settlements caused by deep excavations in Sands", *Geotechnical Engineering Journal of the SEAGS & AGSSEA*, **46**(3), 111-118, ISSN 0046-5828.

EFJV (2015), *Settlement prediction due to diaphragm walls of Heliopolis Station.*, The Egyptian French Joint Venture Co., Cairo metro line -3 technical report, Greater Cairo, Egypt.

PLAXIS, (2016), *Reference Manual*. Plaxis BV Inc., Amsterdam, Netherlands.

Abdel-Rahman, A.H. and El-Sayed, S.M. (2009), "Foundation subsidence due to trenching of diaphragm walls and deep braced excavations in alluvium soils", *Proceedings of the 17th International Conference on Soil Mechanics and Geotechnical Engineering*, Alexandria, Egypt, October.

Aye, Z.Z., Karki, D. and Schulz, C. (2006), "Ground movement prediction and building damage risk-assessment for the deep excavations and tunneling works in Bangkok subsoil", *International Symposium on Underground Excavation and Tunnelling*, Bangkok, Thailand, February.

Korff, M. and Mair, R.J. (2013), "Ground displacements related to deep excavation in Amsterdam", *Proceedings of the 18th International Conference on Soil Mechanics and Geotechnical Engineering*, Paris, France, September.

Feng, Z., Xu, Q., Xu, X., Tang, Q., Li, X. and Liao, X. (2022), "Deformation characteristics of soil layers and diaphragm walls during deep foundation pit excavation: Simulation verification and parameter analysis.", *Symmetry*, **14**(2), 1-14, https://doi.org/10.3390/sym14020254.

Naseri, S., Bahrani, N. (2021), "Design of Initial Shotcrete Lining for a Mine Shaft Using Two-Dimensional Finite Element Models Considering Excavation Advance Rate.", *Geotech. Geol. Eng.*, **39**, 4709–4732. http://doi.org/10.1007/s10706-021-01773-4.

Liu, X., El Naggar, M.H., Wang, K., Tu, Y., Qiu, X. (2021),"Simplified model of defective pile-soil interaction considering three-dimensional effect and application to integrity testing." *Comput. Geotech.*, **132**, 103986. http://doi.org/10.1016/j.compgeo.2020.103986.

Kechidi, S., Colaço, A., Costa, P.A., Castro, J.M., Marques, M. (2021), "Modelling of soil-structure interaction in OpenSees: A practical approach for performance-based seismic design.", *Structures*, **30**, 75–88. http://doi.org/10.1016/j.istruc.2021.01.006.

Zhu, G. (2021), "Mindlin solution on ground deformation caused by the trench excavation during installation of concrete diaphragm wall panels.", *Scientific reports*, **11**(1), 1-16, https://doi.org/10.1038/s41598-021-98403-z.